Mecánica Computacional Vol. XXIV
A. Larreteguy (Editor)
Buenos Aires, Argentina, Noviembre 2005

RESULTS ON TRANSVERSAL AND AXIAL MOTIONS OF A SYSTEM OF TWO BEAMS COUPLED TO A JOINT THROUGH TWO LEGS †

J. A. Burns*, E. M. Cliff*, Z. Liu and R. D. Spies‡**

* Interdisciplinary Center for Applied Mathematics
Virginia Tech, Blacksburg, VA 24061-0531, USA

** Department of Mathematics and Statistics
University of Minnesota at Duluth, Duluth, MN 55812-3000, USA

‡ Instituto de Matemática Aplicada del Litoral, IMAL
CONICET -UNL , Güemes 3450, Santa Fe, Argentina
E-mail: rspies@imalpde.ceride.gov.ar

Key Words: Ordinary Differential Equations, Partial Differential Equations, Mechanics of Deformable Solids.

Abstract. *In recent years there has been renewed interest in inflatable-rigidizable space structures because of the efficiency they offer in packaging during boost-to-orbit.[1] However, much research is still needed to better understand dynamic response characteristics, including inherent damping, of truss structures fabricated with these advanced material systems. We present results of an ongoing research related to a model consisting of an assembly of two beams with Kelvin-Voight damping, coupled to a simple joint through two legs. The beams are clamped at one end but at the other end they satisfy a boundary condition given in terms of an ODE coupling boundary terms of both beams, which reflects geometric compatibility conditions. The system is then written as a second order differential equation in an appropriate Hilbert space in which well-posedness, exponential stability as well as other regularity properties of the solutions can be obtained. Two different finite dimensional approximation schemes for the solutions of the system are presented. Numerical results are presented and comparisons are made.*

† This research was supported in part by Defense Advanced Research Projects Agency/Special Projects Office (DARPA/SPO), NASA Langley Research Center and the National Institute for Aerospace of USA, under Grant NIA 2535, by the Consejo Nacional de Investigaciones Científica y Técnicas of Argentina, CONICET and by Universidad Nacional del Litoral, UNL, Santa Fe, Argentina.

1 INTRODUCTION: THE MODEL

We consider the joint-legs-beams system is depicted in Figure 1. This system arises in the study of the dynamics of cross-sections of the truss-structure depicted in Figure 2. In our model, both beams are clamped at the ends $s_i = 0$, $i = 1, 2$ and can vibrate in the plane. The transverse (bending) deformation of beam i is denoted by $w^i(t, s_i)$ while the longitudinal (axial) deformation is denoted by $u^i(t, s_i)$, where $0 \leq s_i \leq L_i$, $i = 1, 2$. Kelvin-Voight damping is considered for both longitudinal and transverse beam motions. The joint configuration is described by the planar Cartesian displacements of the pivot, denoted by $x(t)$ and $y(t)$ and by $\theta_1(t)$, $\theta_2(t)$, where $\theta_i(t)$ denotes the angle between leg i and positive x axis. The physical parameters and variables used in the model are as follows:

- L_i, A_i, I_i, E_i, ρ_i: length, cross section area, moment of inertia, Young's modulus and mass density of beam i, $i = 1, 2$.
- $x(t)$, $y(t)$: horizontal and vertical displacements of the joint, $t \geq 0$.
- $\theta_i(t)$: angle of leg i with the horizontal, $i = 1, 2$, $t \geq 0$.
- ℓ_i, m_i, I_ℓ^i, d_i: length, mass, moment of inertia about center of mass and distance from pivot to center of mass of leg i, $i = 1, 2$.
- $I_Q^i = I_\ell^i + m_i d_i^2$: moment of inertia of leg i about pivot, $i = 1, 2$.
- μ_i, γ_i, b, k: Kelvin-Voight damping parameters in the axial motions, in the transverse bending, internal viscous joint damping and stiffness parameters.
- m_p: mass of the pivot.
- $m = m_1 + m_2 + m_p$: total mass of the joint system.
- φ_1, φ_2: angles at equilibrium of beam 1 with respect to the positive y axis and of beam 2 with respect to the negative y axis, respectively.
- $F_i(t)$, $N_i(t)$, $M_i(t)$: extensional force, shear force and bending moment at the end $s_i = L_i$ of beam i.
- $M_Q(t)$: internal torque exerted on joint-leg 1 by joint-leg 2.

1.1 Constitutive equations

For the transverse (bending) motions of the beams, an Euler-Bernoulli model with Kelvin-Voight damping is considered, i.e.

$$\rho_i A_i \frac{\partial^2 w^i(t,s_i)}{\partial t^2} + \frac{\partial^2}{\partial s_i^2}\left[E_i I_i \frac{\partial^2 w^i(t,s_i)}{\partial s_i^2} + \gamma_i \frac{\partial^3 w^i(t,s_i)}{\partial s_i^2 \partial t}\right] = 0, \tag{1}$$

$$w^i(t,0) = \frac{\partial w^i(t,0)}{\partial s_i} = 0. \tag{2}$$

The longitudinal (axial) motions of the beams, also with Kelvin-Voight damping, are described by:

$$\rho_i A_i \frac{\partial^2 u^i(t,s_i)}{\partial t^2} - \frac{\partial}{\partial s_i}\left[E_i A_i \frac{\partial u^i(t,s_i)}{\partial s_i} + \mu_i \frac{\partial^2 u^i(t,s_i)}{\partial s_i \partial t}\right] = 0, \tag{3}$$

$$u^i(t,0) = 0. \tag{4}$$

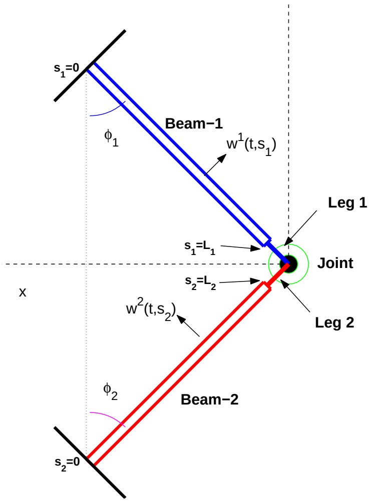

Figure 1: Basic structure of the joint-legs-beams system

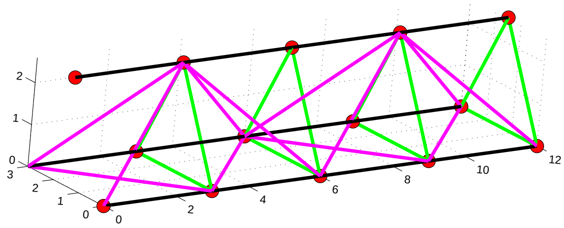

Figure 2: Truss-structure

For the joint-legs, from Newtonian mechanics, we obtain:

$$\begin{aligned}
&m\,\ddot{x}(t) - m_1 d_1 \sin\theta_1(t)\ddot{\theta}_1(t) - m_2 d_2 \sin\theta_2(t)\ddot{\theta}_2(t) \\
&= m_1 d_1 \cos\theta_1(t)\dot{\theta}_1(t)^2 + m_2 d_2 \cos\theta_2(t)\dot{\theta}_2(t)^2 + F_1(t)\cos\theta_1(t) \\
&\quad - N_1(t)\sin\theta_1(t) + F_2(t)\cos\theta_2(t) - N_2(t)\sin\theta_2(t),
\end{aligned} \tag{5}$$

$$\begin{aligned}
&m\,\ddot{y}(t) + m_1 d_1 \cos\theta_1(t)\ddot{\theta}_1(t) + m_2 d_2 \cos\theta_2(t)\ddot{\theta}_2(t) \\
&= m_1 d_1 \sin\theta_1(t)\dot{\theta}_1(t)^2 + m_2 d_2 \sin\theta_2(t)\dot{\theta}_2(t)^2 + F_1(t)\sin\theta_1(t) \\
&\quad + N_1(t)\cos\theta_1(t) + F_2(t)\sin\theta_2(t) + N_2(t)\cos\theta_2(t),
\end{aligned} \tag{6}$$

$$\begin{aligned}
I_Q^1\,\ddot{\theta}_1(t) &= M_Q(t) + M_1(t) + \ell_1\,N_1(t) \\
&\quad + m_1 d_1 \left[\ddot{x}(t)\sin\theta_1(t) - \ddot{y}(t)\cos\theta_1(t)\right],
\end{aligned} \tag{7}$$

$$\begin{aligned}
I_Q^2\,\ddot{\theta}_2(t) &= -M_Q(t) + M_2(t) + \ell_2\,N_2(t) \\
&\quad + m_2 d_2 \left[\ddot{x}(t)\sin\theta_2(t) - \ddot{y}(t)\cos\theta_2(t)\right].
\end{aligned} \tag{8}$$

Since the continuum equations (1)-(4) reflect small deflection theory, we shall consider equations (5)-(8), linearized about $x^0 = y^0 = \dot{x}^0 = \dot{y}^0 = \dot{\theta}_1^0 = \dot{\theta}_1^0 = 0$ and $\theta_1^0 = \frac{\pi}{2} - \varphi_1$, $\theta_2^0 = -\frac{\pi}{2} + \varphi_2$. These equations are:

$$\begin{aligned}
&m\,\ddot{x}(t) - m_1 d_1 \cos\varphi_1 \ddot{\theta}_1(t) + m_2 d_2 \cos\varphi_2 \ddot{\theta}_2(t) \\
&= F_1(t)\sin\varphi_1 - N_1(t)\cos\varphi_1 + F_2(t)\sin\varphi_2 + N_2(t)\cos\varphi_2,
\end{aligned} \tag{9}$$

$$\begin{aligned}
&m\,\ddot{y}(t) + m_1 d_1 \sin\varphi_1 \ddot{\theta}_1(t) + m_2 d_2 \sin\varphi_2 \ddot{\theta}_2(t) \\
&= F_1(t)\cos\varphi_1 + N_1(t)\sin\varphi_1 - F_2(t)\cos\varphi_2 + N_2(t)\sin\varphi_2,
\end{aligned} \tag{10}$$

$$I_Q^1\ddot{\theta}_1(t) = M_Q(t) + M_1(t) + \ell_1\, N_1(t) + m_1 d_1 \left[\ddot{x}(t)\cos\varphi_1 - \ddot{y}(t)\sin\varphi_1\right], \tag{11}$$

$$I_Q^2\ddot{\theta}_2(t) = -M_Q(t) + M_2(t) + \ell_2\, N_2(t) - m_2 d_2 \left[\ddot{x}(t)\cos\varphi_2 + \ddot{y}(t)\sin\varphi_2\right]. \tag{12}$$

It must be noted that in equations (9)-(12), $\theta_i(t)$ denotes the perturbation in the angle between leg i and the positive x axis. Although more generality is possible, in the present formulation we shall consider only linear elastic and viscous effects in the internal moment, assuming therefore $M_Q(t)$ in the form:

$$M_Q(t) = k\left(\theta_2(t) - \theta_1(t)\right) + b\left(\dot{\theta}_2(t) - \dot{\theta}_1(t)\right) \ . \tag{13}$$

1.2 Compatibility conditions

First, geometric compatibility conditions require that the Cartesian position of the beams tip and the joint-legs remain the same, and also that the end-slope of the beam be the same as the slope of the leg. These conditions translate into the following equations.

$$\begin{cases} x(t) - \ell_1\theta_1(t)\cos\varphi_1 + w^1(t,L_1)\cos\varphi_1 + u^1(t,L_1)\sin\varphi_1 = 0 \\ y(t) + \ell_1\theta_1(t)\sin\varphi_1 - w^1(t,L_1)\sin\varphi_1 + u^1(t,L_1)\cos\varphi_1 = 0 \\ \theta_1(t) + w_s^1(t,L_1) = 0 \end{cases} \tag{14}$$

$$\begin{cases} x(t) + \ell_2\theta_2(t)\cos\varphi_2 - w^2(t,L_2)\cos\varphi_2 + u^2(t,L_2)\sin\varphi_2 = 0 \\ y(t) + \ell_2\theta_2(t)\sin\varphi_2 - w^2(t,L_2)\sin\varphi_2 - u^2(t,L_2)\cos\varphi_2 = 0 \\ \theta_2(t) + w_s^2(t,L_2) = 0 \end{cases} \tag{15}$$

These equations can also be written in the form:

$$\begin{cases} u^1(t,L_1) = -x(t)\sin\varphi_1 - y(t)\cos\varphi_1 \\ w^1(t,L_1) = -x(t)\cos\varphi_1 + y(t)\sin\varphi_1 + \ell_1\theta_1(t) \\ w_s^1(t,L_1) = -\theta_1(t) \end{cases} \tag{16}$$

$$\begin{cases} u^2(t,L_2) = -x(t)\sin\varphi_2 + y(t)\cos\varphi_2 \\ w^2(t,L_2) = \ x(t)\cos\varphi_2 + y(t)\sin\varphi_2 + \ell_2\theta_2(t) \\ w_s^2(t,L_2) = -\theta_2(t) \end{cases} \tag{17}$$

Also, the Kelvin-Voight constitutive model requires the following compatibility conditions.

For the bending moments at the interfaces:

$$\begin{cases} E_1 I_1 w_{ss}^1(t,L_1) + \gamma_1 \dot{w}_{ss}^1(t,L_1) = M_1(t) \\ E_2 I_2 w_{ss}^2(t,L_2) + \gamma_2 \dot{w}_{ss}^2(t,L_2) = M_2(t) \end{cases} \tag{18}$$

For the shear forces at the interfaces:

$$\begin{cases} \frac{\partial}{\partial s}\left(E_1 I_1 w_{ss}^1 + \gamma_1 \dot{w}_{ss}^1\right)(t, L_1) = N_1(t) \\ \frac{\partial}{\partial s}\left(E_2 I_2 w_{ss}^2 + \gamma_2 \dot{w}_{ss}^2\right)(t, L_2) = N_2(t) \end{cases} \tag{19}$$

For the axial forces at the interfaces:

$$\begin{cases} \frac{\partial}{\partial s}\left(E_1 A_1 u^1 + \mu_1 \dot{u}^1\right)(t, L_1) = F_1(t) \\ \frac{\partial}{\partial s}\left(E_2 A_2 u^2 + \mu_2 \dot{u}^2\right)(t, L_2) = F_2(t) \end{cases} \tag{20}$$

The apparently cumbersome notation for spatial derivatives in equations (19) and (20) is necessary because although the sums in each parentheses are smooth, each one of the summands need not be (see for instance[3] and[4]).

2 ENERGY EQUATIONS AND THE DISSIPATIVENESS OF THE SYSTEM

Multiplying equations (1) by $\dot{w}(t,s)$, integrating by parts and using boundary conditions (2) and compatibility conditions (18) and (19), we obtain for each beam an equation of the form

$$\begin{aligned} 0 &= \frac{d}{dt}\left\{\frac{1}{2}\int_0^L \left[\rho A(\dot{w})^2 + EI(w_{ss})^2\right]\, ds\right\} + \dot{w}(t,L)N(t) - \dot{w}_s(t,L)M(t) + \gamma \int_0^L \dot{w}_{ss}^2\, ds \\ &= \frac{d}{dt}E(\text{beam} - w) + \dot{w}(t,L)N(t) - \dot{w}_s(t,L)M(t) \;+\; \gamma \int_0^L \left(\dot{w}_{ss}\right)^2\, ds, \end{aligned} \tag{21}$$

where $E(\text{beam} - w)$ is the energy of the beam due to transverse motions, defined as

$$E(\text{beam} - w) \doteq \frac{1}{2}\int_0^L \left[\rho A(\dot{w})^2 + EI(w_{ss})^2\right]\, ds. \tag{22}$$

Now, using equations (16) and (17) to replace $\dot{w}(t,L)$ and $\dot{w}_s(t,L)$ in (21) and adding together the equations for both beams we obtain

$$\begin{aligned} 0 &= \frac{d}{dt}\left[E(\text{beam} - w^1) + E(\text{beam} - w^2)\right] + \gamma_1 \int_0^{L_1} \left(\dot{w}_{ss}^1\right)^2\, ds + \gamma_2 \int_0^{L_2} \left(\dot{w}_{ss}^2\right)^2\, ds \\ &+ \dot{\theta}_1(t)M_1(t) + \dot{\theta}_2(t)M_2(t) + N_1(t)\left[\ell_1\dot{\theta}_1(t) - \dot{x}(t)\cos\varphi_1 + \dot{y}(t)\sin\varphi_1\right] \\ &+ N_2(t)\left[\ell_2\dot{\theta}_2(t) + \dot{x}(t)\cos\varphi_2 + \dot{y}(t)\sin\varphi_2\right]. \end{aligned} \tag{23}$$

Similarly, multiplying equations (3) by $\dot{u}$, integrating by parts and using boundary conditions (4) and compatibility conditions (20) we obtain for each beam an equation of the form

$$\begin{aligned} 0 &= \frac{d}{dt}\left\{\frac{1}{2}\int_0^L \left[\rho A(\dot{u})^2 + EA(u_s)^2\right]\, ds\right\} - \dot{u}(t,L)\frac{\partial}{\partial s}\left[EAu(t,L) - \mu\dot{u}(t,L)\right] \\ &+ \mu\int_0^L \left(\dot{u}_s\right)^2\, ds \;=\; \frac{d}{dt}E(\text{beam} - u) - \dot{u}(t,L)F(t) + \mu\int_0^L \left(\dot{u}_s\right)^2\, ds, \end{aligned} \tag{24}$$

where $E(\text{beam} - u)$ is the energy of the beam due to longitudinal motions, defined as

$$E(\text{beam} - u) \doteq \frac{1}{2}\int_0^L \left[\rho A(\dot{u})^2 + EA(u_s)^2\right] \, ds. \tag{25}$$

Now, adding together the equations for both beams and using equations (16) and (17) to replace $\dot{u}^1(t, L_1)$ and $\dot{u}^2(t, L_2)$ we obtain

$$\begin{aligned} 0 &= \frac{d}{dt}\left[E(\text{beam} - u^1) + E(\text{beam} - u^2)\right] + \mu_1 \int_0^{L_1} \left(\dot{u}_s^1\right)^2 \, ds + \mu_2 \int_0^{L_2} \left(\dot{u}_s^2\right)^2 \, ds \\ &+ F_1(t)\left[\dot{x}(t)\sin\varphi_1 + \dot{y}(t)\cos\varphi_1\right] + F_2(t)\left[\dot{x}(t)\sin\varphi_2 - \dot{y}(t)\cos\varphi_2\right]. \end{aligned} \tag{26}$$

Now we multiply equations (9), (10), (11), (12) by $\dot{x}(t)$, $\dot{y}(t)$, $\dot{\theta}_1(t)$ and $\dot{\theta}_2(t)$, respectively, and add them together to obtain

$$\begin{aligned} 0 &= \frac{d}{dt}\frac{1}{2}\Big[m\left((\dot{x}(t))^2 + (\dot{y}(t))^2\right. + I_Q^1(\dot{\theta}_1(t))^2 + I_Q^2(\dot{\theta}_2(t))^2 \\ &+ \dot{x}(t)\Big(-m_1 d_1 \cos\varphi_1 \ddot{\theta}_1(t) + m_2 d_2 \cos\varphi_2 \ddot{\theta}_2(t) - F_1(t)\sin\varphi_1 \\ &\qquad + N_1(t)\cos\varphi_1 - F_2(t)\sin\varphi_2 - N_2(t)\cos\varphi_2\Big) \\ &+ \dot{y}(t)\Big(m_1 d_1 \sin\varphi_1 \ddot{\theta}_1(t) + m_2 d_2 \sin\varphi_2 \ddot{\theta}_2(t) - F_1(t)\cos\varphi_1 \\ &\qquad - N_1(t)\sin\varphi_1 + F_2(t)\cos\varphi_2 - N_2(t)\sin\varphi_2\Big) \\ &+ \dot{\theta}_1(t)\left(-M_Q(t) - M_1(t) - \ell_1 N_1(t) - m_1 d_1 \ddot{x}(t)\cos\varphi_1 + m_1 d_1 \ddot{y}(t)\sin\varphi_1\right) \\ &+ \dot{\theta}_2(t)\left(M_Q(t) - M_2(t) - \ell_2 N_2(t) + m_2 d_2 \ddot{x}(t)\cos\varphi_2 + m_2 d_2 \ddot{y}(t)\sin\varphi_2\right). \end{aligned} \tag{27}$$

Adding together equations (23), (26) and (27) we obtain

$$\begin{aligned} &\frac{d}{dt}\Big\{E(\text{beam} - w^1) + E(\text{beam} - w^2) + E(\text{beam} - u^1) + E(\text{beam} - u^2) \\ &\qquad + m\left((\dot{x}(t))^2 + (\dot{y}(t))^2\right) + I_Q^1(\dot{\theta}_1(t))^2 + I_Q^2(\dot{\theta}_2(t))^2\Big] \\ &\qquad + m_1 d_1\left(-\dot{x}(t)\dot{\theta}_1(t)\cos\varphi_1 + \dot{y}(t)\dot{\theta}_1(t)\sin\varphi_1\right) \\ &\qquad + m_2 d_2\left(\dot{x}(t)\dot{\theta}_2(t)\cos\varphi_2 + \dot{y}(t)\dot{\theta}_2(t)\sin\varphi_2\right)\Big\} \\ &= -\gamma_1 \int_0^{L_1} \left(\dot{w}_{ss}^1\right)^2 \, ds - \gamma_2 \int_0^{L_2} \left(\dot{w}_{ss}^2\right)^2 \, ds \\ &- \mu_1 \int_0^{L_1} \left(\dot{u}_s^1\right)^2 \, ds - \mu_2 \int_0^{L_2} \left(\dot{u}_s^2\right)^2 \, ds - M_Q(t)[\dot{\theta}_2(t) - \dot{\theta}_1(t)]. \end{aligned} \tag{28}$$

Recalling now that $M_Q(t) = k[\theta_2(t) - \theta_1(t)] + b[\dot\theta_2(t) - \dot\theta_1(t)]$ (see equation (13)), $I_Q^i = I_\ell^i + m_i d_i^2$, $i = 1,\, 2$, and that $m = m_1 + m_2 + m_p$, equation (28) above can be written as

$$\frac{d}{dt}\left\{E(\text{beam} - w^1) + E(\text{beam} - w^2) + E(\text{beam} - u^1) + E(\text{beam} - u^2) + E(\text{joint-legs})\right\}$$
$$= -\gamma_1 \int_0^{L_1} \left(\dot w_{ss}^1\right)^2\, ds - \gamma_2 \int_0^{L_2} \left(\dot w_{ss}^2\right)^2\, ds$$
$$- \mu_1 \int_0^{L_1} \left(\dot u_s^1\right)^2\, ds - \mu_2 \int_0^{L_2} \left(\dot u_s^2\right)^2\, ds - b[\dot\theta_2(t) - \dot\theta_1(t)]^2, \tag{29}$$

where

$$\begin{aligned}
2\, E(\text{joint-legs}) &\doteq m\left((\dot x(t))^2 + (\dot y(t))^2 \right) + I_Q^1(\dot\theta_1(t))^2 + I_Q^2(\dot\theta_2(t))^2 \\
&\quad + m_1 d_1 \left(-\dot x(t)\dot\theta_1(t)\cos\varphi_1 + \dot y(t)\dot\theta_1(t)\sin\varphi_1\right) \\
&\quad + m_2 d_2 \left(\dot x(t)\dot\theta_2(t)\cos\varphi_2 + \dot y(t)\dot\theta_2(t)\sin\varphi_2\right) + k\left(\theta_2(t) - \theta_1(t)\right)^2 \\
&= m_1\left(\dot x(t) - d_1\dot\theta_1(t)\cos\varphi_1\right)^2 + m_2\left(\dot y(t) + d_1\dot\theta_1(t)\sin\varphi_1\right)^2 \\
&\quad + m_1\left(\dot x(t) + d_2\dot\theta_2(t)\cos\varphi_2\right)^2 + m_2\left(\dot y(t) + d_2\dot\theta_2(t)\sin\varphi_2\right)^2 \\
&\quad + m_p\left(\dot x(t)^2 + \dot y(t)^2\right) + I_\ell^1\dot\theta_1(t)^2 + I_\ell^2\dot\theta_2(t)^2 + k\left(\theta_2(t) - \theta_1(t)\right)^2 .
\end{aligned} \tag{30}$$

Note that by (29), if $\gamma_1 = \gamma_2 = \mu_1 = \mu_2 = b = 0$ then the system is conservative and it is dissipative otherwise.

In Burns et all,[5] system (1)-(17) was written as a second order differential equation of the form $\ddot X(t) + \mathcal{A}\left(S\dot X(t) + X(t)\right) = 0$, in an appropriate Hilbert space $\mathcal{H}$. This space is a product of spaces describing the distributed beam deflections and a finite dimensional space that projects important features at the joint boundary. In this context, the total energy of the system, i.e. the expression within brackets in the left hand side of (29), takes the form $E(X, \dot X) = \frac{1}{2}\left(||\dot X(t)||_{\mathcal{H}}^2 + ||\mathcal{A}^{\frac{1}{2}} X(t)||_{\mathcal{H}}^2\right)$. Also, using this abstract framework, the well-posedness of the system was proved and it was shown that solutions decay exponentially in the case in which the damping parameters γ_1, γ_2, μ_1, μ_2 are all strictly positive. A characterization of the spectrum was also given.

3 FINITE DIMENSIONAL APPROXIMATIONS

In this section we will develop finite dimensional approximations for the solutions of system (1)-(17).

3.1 A Projection Method

Transverse motions of the beams. We use a Galerkin procedure with cubic splines to approximate $w^i(t, s_i)$ by $\sum_{j=1}^{n_\omega} z_j^i(t) b_j^i(s_i)$, $i = 1, 2$, $0 \le s_i \le L_i$. Here the b_j^1's and the b_j^2's are cubic splines in $[0, L_1]$ and $[0, L_2]$ respectively, modified as to satisfy the boundary conditions (2), $w^i(t,0) = w^i_{s_i}(t,0) = 0$, i.e. the b^i_j's satisfy $b^i_j(0) = {b^i_j}'(0) = 0$, $j = 1, 2, \dots n_w$, $i = 1, 2$. The weak formulation of equation (1) for each one of the beams, after integration by parts leads to:

$$\begin{aligned} \rho A \int_0^L w_{tt}(t,s)\phi(s)\, ds + EI \int_0^L w_{ss}(t,s)\phi_{ss}(s)\, ds + \gamma \int_0^L w_{sst}(t,s)\phi_{ss}(s)\, ds \\ = EI w_{ss}(t,L)\phi_s(L) - EI w_{sss}(t,L)\phi(L) + \gamma w_{sst}(t,L)\phi_s(L) - \gamma w_{ssst}(t,L)\phi(L) \\ = \phi_s(L)\left[EI w_{ss}(t,L) + \gamma w_{sst}(t,L)\right] - \phi(L)\left[EI w_{sss}(t,L) + \gamma w_{ssst}(t,L)\right] \\ = \phi_s(L)M(t) - \phi(L)N(t) \qquad \text{(by virtue of equations (18) and (19))}, \end{aligned}$$

where the ϕ's are test functions. Using the same cubic splines as test functions, the above equation can be written in matrix form as

$$\rho A M^b \ddot{z}(t) + EI H^b z(t) + \gamma H^b \dot{z}(t) = b'(L)M(t) - b(L)N(t),$$

where $z(t) = (z_1(t), z_2(t), \dots, z_{n_\omega}(t))^T$, $b(s) = (b_1(s), b_2(s), \dots, b_{n_\omega}(s))^T$, and M^b, H^b are the matrices given by $M^b = \left(\int_0^L b_j(s) b_k(s)\, ds\right)$, $H^b = \left(\int_0^L b''_j(s) b''_k(s)\, ds\right)$.

We have one equation like this for each beam. We write these equations in the form:

$$\rho_1 A_1 M_1^b \ddot{z}^1(t) + E_1 I_1 H_1^b z^1(t) + \gamma_1 H_1^b \dot{z}^1(t) = {b^1}'(L_1) M_1(t) - b^1(L_1) N_1(t),$$

$$\rho_2 A_2 M_2^b \ddot{z}^2(t) + E_2 I_2 H_2^b z^2(t) + \gamma_2 H_2^b \dot{z}^2(t) = {b^2}'(L_2) M_2(t) - b^2(L_2) N_2(t).$$

By denoting with $z(t)$ the finite dimensional state variable for the transverse motions of both beams, $z(t) \doteq \begin{pmatrix} z^1(t) \\ z^2(t) \end{pmatrix}$, the above two equations can be written as

$$M_w \ddot{z}(t) = A_w z(t) + B_w \dot{z}(t) + C_w \begin{pmatrix} M_1(t) \\ N_1(t) \\ M_2(t) \\ N_2(t) \end{pmatrix}, \tag{31}$$

where

$$M_w \doteq \begin{pmatrix} \rho_1 A_1 M_1^b & \mathbf{0} \\ \mathbf{0} & \rho_2 A_2 M_2^b \end{pmatrix}, \qquad A_w \doteq \begin{pmatrix} -E_1 I_1 H_1^b & \mathbf{0} \\ \mathbf{0} & -E_2 I_2 H_2^b \end{pmatrix}, \tag{32}$$

$$B_w \doteq \begin{pmatrix} -\gamma_1 H_1^b & \mathbf{0} \\ \mathbf{0} & -\gamma_2 H_2^b \end{pmatrix}, \qquad C_w \doteq \begin{pmatrix} {b^1}'(L_1) & -b^1(L_1) & \mathbf{0} & \mathbf{0} \\ \mathbf{0} & \mathbf{0} & {b^2}'(L_2) & -b^2(L_2) \end{pmatrix}. \tag{33}$$

Longitudinal motions of the beams. We now proceed to do the same for the longitudinal displacements of the beams. After integration by parts, and using the boundary conditions (4) at $s = 0$, the weak formulation of equation (3)for each one of the beams takes the form:

$$\begin{aligned} 0 &= \rho A \int_0^L u_{tt}(t,s)\phi(s)\,ds + EA\int_0^L u_s(t,s)\phi_s(s)\,ds + \mu \int_0^L u_{st}(t,s)\phi_s(s)\,ds \\ &= EAu_s(t,L)\phi(L) + \mu u_{st}(t,L)\phi(L) \\ &= F(t)\phi(L) \qquad\qquad \text{(by virtue of the compatibility conditions (20))}, \end{aligned}$$

where the ϕ's are test functions. We approximate the longitudinal displacements $u^i(t,s_i)$ of each beam by by $\sum_{j=1}^{n_u} r_j^i(t) l_j^i(s_i)$, $i = 1,2$, $0 \le s_i \le L_i$. Here the l_j^1's and the l_j^2's are linear splines in $[0, L_1]$ and $[0, L_2]$, respectively, modified as to satisfy the boundary conditions (4), i.e. the l_j^i's satisfy $l_j^i(0) = 0$, $j = 1,2,\ldots,n_u$, $i = 1,2$. Using the same linear splines as test functions, the equation above can be written in the form $\rho AM^\ell \ddot r(t) + EAK^\ell r(t) + \mu K^\ell \dot r(t) = l(L)F(t)$, where $r(t) \doteq (r_1(t), r_2(t), \ldots, r_{n_u}(t))^T$, $l(s) \doteq (l_1(s), l_2(s), \ldots, l_{n_u}(s))^T$, and M^ℓ, K^ℓ are the mass and stiffness matrices given by $M^\ell \doteq \left(\int_0^L \ell_j(s)\ell_k(s)\,ds\right)$, $K^\ell \doteq \left(\int_0^L l'_j(s) l'_k(s)\,ds\right)$.

We have an equation like this for each beam. We write them in the form

$$\rho_1 A_1 M_1^\ell \ddot r^1(t) + E_1 A_1 K_1^\ell r^1(t) + \mu_1 K_1^\ell \dot r_1(t) = l^1(L_1)F_1(t),$$

$$\rho_2 A_2 M_2^\ell \ddot r^2(t) + E_2 A_2 K_2^\ell r^2(t) + \mu_2 K_2^\ell \dot r_2(t) = l^2(L_2)F_2(t).$$

By denoting with $r(t)$ the finite dimensional state variable for the longitudinal motions of both beams, $r(t) \doteq \begin{pmatrix} r^1(t) \\ r^2(t) \end{pmatrix}$, the above two equations can be written as

$$M_u \ddot r(t) = A_u r(t) + B_u \dot r(t) + C_u \begin{pmatrix} F_1(t) \\ F_2(t) \end{pmatrix}, \tag{34}$$

where

$$M_u \doteq \begin{pmatrix} \rho_1 A_1 M_1^\ell & \mathbf{0} \\ \mathbf{0} & \rho_2 A_2 M_2^\ell \end{pmatrix}, \qquad A_u \doteq \begin{pmatrix} -E_1 A_1 K_1^\ell & \mathbf{0} \\ \mathbf{0} & -E_2 A_2 K_2^\ell \end{pmatrix}, \tag{35}$$

$$B_u \doteq \begin{pmatrix} -\mu_1 K_1^\ell & \mathbf{0} \\ \mathbf{0} & -\mu_2 K_2^\ell \end{pmatrix}, \qquad C_u \doteq \begin{pmatrix} l^1(L_1) & \mathbf{0} \\ \mathbf{0} & l^2(L_2) \end{pmatrix}. \tag{36}$$

State equations for the joint-legs. We define the state variable for the joint-legs system to be $\eta(t) \doteq \begin{pmatrix} x(t) & y(t) & \theta_1(t) & \theta_2(t) \end{pmatrix}^T$. The linearized equations (9), (10), (11), (12), with M_Q as in (13), can then be written in matrix form as

$$M_\eta \ddot\eta(t) = A_\eta \eta(t) + B_\eta\, \dot\eta(t) + C_\eta F(t), \tag{37}$$

where

$$M_\eta \doteq \begin{pmatrix} mI_2 & P \\ P^T & \mathrm{diag}(I_Q^1, I_Q^2) \end{pmatrix}, \quad \text{with } P \doteq \begin{pmatrix} -m_1 d_1 \cos\varphi_1 & m_2 d_2 \cos\varphi_2 \\ & \\ m_1 d_1 \sin\varphi_1 & m_2 d_2 \sin\varphi_2 \end{pmatrix}, \tag{38}$$

and

$$A_\eta \doteq \begin{pmatrix} 0 & 0 & 0 & 0 \\ 0 & 0 & 0 & 0 \\ 0 & 0 & -k & k \\ 0 & 0 & k & -k \end{pmatrix}, \qquad B_\eta \doteq \begin{pmatrix} 0 & 0 & 0 & 0 \\ 0 & 0 & 0 & 0 \\ 0 & 0 & -b & b \\ 0 & 0 & b & -b \end{pmatrix}, \tag{39}$$

$$F(t) \doteq \begin{pmatrix} M_1(t) \\ N_1(t) \\ M_2(t) \\ N_2(t) \\ F_1(t) \\ F_2(t) \end{pmatrix}, \qquad \text{and} \qquad C_\eta \doteq [C_{\eta,1} \;\; C_{\eta,2}], \tag{40}$$

with

$$C_{\eta,1} \doteq \begin{pmatrix} 0 & -\cos\varphi_1 & 0 & \cos\varphi_2 \\ 0 & \sin\varphi_1 & 0 & \sin\varphi_2 \\ 1 & l_1 & 0 & 0 \\ 0 & 0 & 1 & l_2 \end{pmatrix} \quad \text{and} \quad C_{\eta,2} \doteq \begin{pmatrix} \sin\varphi_1 & \sin\varphi_2 \\ \cos\varphi_1 & -\cos\varphi_2 \\ 0 & 0 \\ 0 & 0 \end{pmatrix}. \tag{41}$$

State equations for the completely discretized beams-joint-legs system. We define now our discretized state variable for the complete beams-legs-joint system to be $Z(t) \doteq (z(t),\; r(t),\; \eta(t))^T$, and let $n \doteq 2(n_\omega + n_u) + 4$. Equations (31), (34) and (37) can then be written in terms of $Z(t)$ in the form

$$M\ddot{Z}(t) \;=\; AZ(t) + B\dot{Z}(t) + CF(t), \tag{42}$$

where M, A and B are $n \times n$ mass, stiffness and damping matrices, respectively, and C is an $n \times 6$ matrix defined by

$$M \doteq \begin{pmatrix} M_w & \mathbf{0} & \mathbf{0} \\ \mathbf{0} & M_u & \mathbf{0} \\ \mathbf{0} & \mathbf{0} & M_\eta \end{pmatrix}, \quad A \doteq \begin{pmatrix} A_w & \mathbf{0} & \mathbf{0} \\ \mathbf{0} & A_u & \mathbf{0} \\ \mathbf{0} & \mathbf{0} & A_\eta \end{pmatrix}, \quad B \doteq \begin{pmatrix} B_w & \mathbf{0} & \mathbf{0} \\ \mathbf{0} & B_u & \mathbf{0} \\ \mathbf{0} & \mathbf{0} & B_\eta \end{pmatrix}, \quad C \doteq \begin{pmatrix} C_w & \mathbf{0} \\ \mathbf{0} & C_u \\ C_{\eta,1} & C_{\eta,2} \end{pmatrix}. \tag{43}$$

Next, using the recently introduced finite dimensional Galerkin approximations for $w^i(t, s_i)$ and $u^i(t, s_i)$, $i = 1, 2$, it turns out that the geometric compatibility conditions (equations (16) and (17)), can be writen, in an appropriate order, in the form:

$$G \begin{pmatrix} z^1(t) \\ z^2(t) \\ r^1(t) \\ r^2(t) \\ \eta(t) \end{pmatrix} \;=\; G\,Z(t) \;=\; \mathbf{0}, \tag{44}$$

where G is the matrix $G \doteq \begin{pmatrix} C_w^T & \mathbf{0} & C_{\eta,1}^T \\ \\ \mathbf{0} & C_u^T & C_{\eta,2}^T \end{pmatrix}$. We then observe that this matrix G is exactly the transposed of the matrix C defined in (43) and therefore, the compatibility equation (44) above simply takes the form

$$C^T Z(t) = \mathbf{0}. \tag{45}$$

Finally, the completely discretized system of equations consists then of the non-homogeneous system of n second order ODE's (42) plus the differential-algebraic compatibility conditions given by equation (45), i.e

$$\begin{cases} M\ddot{Z}(t) = AZ(t) + B\dot{Z}(t) + CF(t) \\ C^T Z(t) = 0. \end{cases} \tag{46}$$

Note that C^T is a non-square $6 \times n$ matrix.

3.1.1 Enforcing the constraint $C^T Z(t) = 0$ into the dynamic equations

The question that immediately arises is how to actually solve system (46). We proceed now to develop two different methods to accomplish this goal. Multiplying the first equation in (46) first by $C^T M^{-1}$ and then using the second equation in its second order differential form, we obtain

$$\begin{aligned} CF(t) &= -C\left(C^T M^{-1} C\right)^{-1} C^T M^{-1}\left(AZ(t) + B\dot{Z}(t)\right) \\ &= -\hat{\mathcal{P}}\left(AZ(t) + B\dot{Z}(t)\right), \end{aligned} \tag{47}$$

where

$$\hat{\mathcal{P}} \doteq C\left(C^T M^{-1} C\right)^{-1} C^T M^{-1}. \tag{48}$$

One can immediately verify that $\hat{\mathcal{P}}$ is the orthogonal projection of $\mathbb{R}^n$ onto the orthogonal complement of the null space of $C^T M^{-1}$ or, equivalently onto the preimage under M of the range of C, i.e. $\hat{\mathcal{P}} \;:\; \mathbb{R}^n \xrightarrow{\perp} \mathcal{N}(C^T M^{-1})^{\perp} = \mathcal{R}(M^{-1}C) = M^{-1}\mathcal{R}(C)$.

Note: The invertibility of the matrix $C^T M^{-1} C$ above is an immediate consequence of the fact that M, being a mass matrix (more precisely diagonal of mass matrices), is symmetric and positive definite (so M^{-1} has the same properties) and the matrix C^T has full rank. This implies that $\mathcal{N}(C^T M^{-1} C) \;=\; \mathcal{N}(C) = \{0\}$.

Replacing with (47) and (48) into (46) we obtain

$$M\ddot{Z}(t) \;=\; (\mathcal{I} - \hat{\mathcal{P}})\left(AZ(t) + B\dot{Z}(t)\right) \;=\; \mathcal{P}\left(AZ(t) + B\dot{Z}(t)\right), \tag{49}$$

where $\mathcal{P} \doteq I - \hat{\mathcal{P}} = I - C(C^T M^{-1} C)^{-1} C^T M^{-1}$ is the orthogonal projection onto the null space of $C^T M^{-1}$ or equivalently, onto the image under M of the null space of C^T, i.e.

$$\mathcal{P} \;:\; \mathrm{I\!R}^n \xrightarrow{\perp} \mathcal{N}(C^T M^{-1}) = M\mathcal{N}(C^T).$$

Written in first order form, equation (49) takes the form

$$\frac{d}{dt}\begin{pmatrix} Z(t) \\ \dot{Z}(t) \end{pmatrix} \;=\; \begin{pmatrix} \mathbf{0} & I \\ M^{-1}\mathcal{P}A & M^{-1}\mathcal{P}B \end{pmatrix} \begin{pmatrix} Z(t) \\ \dot{Z}(t) \end{pmatrix}. \tag{50}$$

Observation This approach can be easily generalized to the case in which the algebraic constraint in (46) is replaced by $\hat{C}Z(t) = 0$ where $\hat{C}$ is an arbitrary $k \times n$ matrix ($k < n$), and it also carries over to the infinite dimensional case.

3.1.2 Another way of enforcing an algebraic constraint: state projection into the null space of the constraint operator

Let us consider once again the system (46) with an arbitrary full-rank constraint operator F : $\mathrm{I\!R}^n \to \mathrm{I\!R}^k$ ($k < n$):

$$\begin{cases} \ddot{M}z(t) = Az(t) + B\dot{z}(t) + Cg(t) \\ Fz(t) = 0 \end{cases}$$

Here $g : [0, \infty) \to \mathrm{I\!R}^k$, C is an $n \times k$ matrix and A, B and M are as in (46). By applying FM^{-1} to the first equation, assuming invertibility of $FM^{-1}C$ and enforcing the second order differential form of the constraint equation, we find as before that $g(t)$ is uniquely determined from $z(t)$ and A, B, C and F. More precisely, $g(t) \;=\; (FM^{-1}C)^{-1}FM{-}1\,(Az(t) + B\dot{z}(t))$, and therefore $M^{-1}Cg(t) \;=\; -\mathcal{P}^* M^{-1}\,(Az(t) + B\dot{z}(t))$, where $\mathcal{P}^* \doteq M^{-1}C(FM^{-1}C)^{-1}F \;=\; F^T(FF^T)^{-1}F$, is the orthogonal projection of $\mathrm{I\!R}^n$ onto the orthogonal complement of the kernel on F, i.e. $\mathcal{P}^* : \mathrm{I\!R}^n \xrightarrow{\perp} [\mathcal{N}(F)]^\perp$. Note that $\mathcal{P}^*$ is independent of C for any C for which $FM^{-1}C$ is invertible. Hence, the dynamic equation becomes

$$\ddot{z}(t) \;=\; (I - \mathcal{P}^*)\,M^{-1}\,(Az(t) + B\dot{z}(t)) \;=\; \mathcal{P}\,M^{-1}\,(Az(t) + B\dot{z}(t)),$$

where $\mathcal{P} \doteq I - \mathcal{P}^* = \; I - F^T(FF^T)^{-1}F$ is the orthogonal projection of $\mathrm{I\!R}^n$ onto $\mathcal{N}(F)$. Now, for any $z \in H$ we write $z = z_1 \oplus z_2$, with $z_1 \in \mathcal{N}(F)$ and $z_2 \in [\mathcal{N}(F)]^\perp$. Using this decomposition and enforcing now the constraint $Fz(t) = 0$ we obtain $z_2(t) = 0$, $z(t) = z_1(t) = \mathcal{P}z(t)$, and

$$\begin{aligned} \ddot{z}(t) \;&=\; \mathcal{P}\,M^{-1}\big(A\,z(t) + B\,\dot{z}(t)\big) \\ &=\; \big[I - F^T(FF^T)^{-1}F\big]\,M^{-1}\,(A\,z(t) + B\,\dot{z}(t)), \end{aligned}$$

or, written in first order form

$$\frac{d}{dt}\begin{pmatrix} z(t) \\ \\ \dot{z}(t) \end{pmatrix} \;=\; \mathcal{A}\begin{pmatrix} z(t) \\ \dot{z}(t) \end{pmatrix},$$

where

$$\mathcal{A} \;\doteq\; \begin{pmatrix} \mathbf{0} & I \\ \\ \mathcal{P}M^{-1}A & \mathcal{P}M^{-1}B \end{pmatrix}.$$

By performing row operations, it can be immediately seen that

$$\det\left[\lambda I - \mathcal{A}\right] \;=\; \det\left[\lambda^2 I - \lambda \mathcal{P}M^{-1}B - \mathcal{P}M^{-1}A\right].$$

Note that in the case of no damping ($B = \mathbf{0}$), the eigenvalues of $\mathcal{A}$ are the square roots of the eigenvalues of $\mathcal{P}M^{-1}A$. Since A is negative definite, M^{-1} positive definite and $\mathcal{P}$ is a projection, $\mathcal{P}M^{-1}A$ is negative semidefinite and its eigenvalues are all real and less or equal than zero. Therefore their square roots are all purely imaginary.

3.2 A Geometric Approach: enforcing the geometric compatibility conditions into the basis functions

In this section we will follow a second approach in which the basis functions for the finite dimensional approximations of the solutions of our system are constructed in such a way as to satisfy the geometric compatibility conditions. Given a length L and an integer $N > 1$ we construct the (uniform) grid $\mathcal{G}(L,N) = \left\{ s_j = \frac{(j-1)}{(N-1)}L \mid j = 1, 2, \ldots, N \right\}$. Let $l_j^{\mathcal{G}}$ be the standard, continuous linear spline on the grid $\mathcal{G}$, such that $l_j^{\mathcal{G}}(s_k) = \delta_{j\,k}$, and consider the set of spline functions $S_1^{\mathcal{G}(L,N)} = \left\{ l_j^{\mathcal{G}} \mid j = 2, \ldots, N \right\}$. The linear span of $S_1^{\mathcal{G}}$ is an $(N-1)$ dimensional subspace of H_0^1. In a similar way we construct a set of cubic splines to approximate H_0^2, including the requirement that $w(0) = w'(0) = 0$. Suppressing details we consider the set $S_3^{\mathcal{G}(L,N)} = \left\{ b_j^{\mathcal{G}} \mid j = 1, \ldots, N \right\}$. The linear span of $S_3^{\mathcal{G}}$ is an N dimensional subspace of H_0^2.

The axial and transverse deflections i^{th} beam are approximated by

$$u^i(t,s_i) = \sum_{j=2}^{N_i^u} p_j^i(t) l_j^{\mathcal{G}(L_i,N_i^u)}(s_i)\,, \qquad w^i(t,s_i) = \sum_{j=2}^{N_i^w} q_j^i(t) b_j^{\mathcal{G}(L_i,N_i^w)}(s_i) \quad \text{respectively.}$$

It's clear that the span of the set

$$S^{\mathcal{G}} \doteq S_3^{\mathcal{G}(L_1,N_1^w)} \otimes S_3^{\mathcal{G}(L_2,N_2^w)} \otimes S_1^{\mathcal{G}(L_1,N_1^u)} \otimes S_1^{\mathcal{G}(L_2,N_2^u)} \otimes \{\mathbf{e}_\imath,\ \imath = 1, \ldots, 4\}\,,$$

is a $N_1^w + N_2^w + N_1^u + N_2^u + 2$ dimensional subspace of the *unconstrained configuration* space

$$\mathcal{H}_u \doteq H_0^2(0,L_1) \times H_0^2(0,L_2) \times H_0^1(0,L_1) \times H_0^1(0,L_2) \times \mathbb{R}^4\,,$$

but is not a subspace of the configuration space that includes the geometric constraints (16)-(17). It can be noted that all but twelve of the basis elements in $S^{\mathcal{G}}$ satisfy (16)-(17) trivially, but that the constraint is not satisfied by the last linear spline in $S_1^{\mathcal{G}}$ (two beams), nor by the last three cubic splines in $S_3^{\mathcal{G}}$ (again, two beams), nor by the basis for $\mathbb{R}^4$. Before proceeding we simplify the presentation by choosing $N_1^w = N_2^w = N_1^u = N_2^u = N$. Also, in order to keep the notation short we shall use the notation $b_j^{(i)}$ and $l_j^{(i)}$ for $b_j^{\mathcal{G}(L_i,N)}$ and $l_j^{\mathcal{G}(L_i,N)}$, respectively. We denote the twelve *nonconforming* basis elements by

$$\xi_k = \begin{bmatrix} 0 \\ 0 \\ 0 \\ 0 \\ \mathbf{e}_k \end{bmatrix} \quad k = 1, \ldots 4 \ , \qquad \xi_5 = \begin{bmatrix} 0 \\ 0 \\ l_N^{(1)} \\ 0 \\ 0 \end{bmatrix} \qquad \xi_6 = \begin{bmatrix} 0 \\ 0 \\ 0 \\ l_N^{(2)} \\ 0 \end{bmatrix} \ ,$$

and

$$\xi_k = \begin{bmatrix} b_{N-(9-k)}^{(1)} \\ 0 \\ 0 \\ 0 \\ 0 \end{bmatrix} \quad k = 7, 8, 9 \ , \qquad \xi_k = \begin{bmatrix} 0 \\ b_{N-(12-k)}^{(2)} \\ 0 \\ 0 \\ 0 \end{bmatrix} \quad k = 10, 11, 12 \ .$$

To impose the geometric constraints (16)-(17) we define the (geometric-constraint) operator $\mathcal{C} : \mathcal{H}_u \mapsto \mathbb{R}^6$ by

$$\mathcal{C} \begin{bmatrix} w^1 \\ w^2 \\ u^1 \\ u^2 \\ \eta \end{bmatrix} \doteq \begin{bmatrix} -w_s^1(L) \\ w^1(L) \\ -w_s^2(L) \\ w^2(L) \\ -u^1(L) \\ -u^2(L) \end{bmatrix} - C_\eta^T \ \eta \ = P_1^B \begin{bmatrix} w^1 \\ w^2 \\ u^1 \\ u^2 \end{bmatrix} - C_\eta^T \ \eta, \tag{51}$$

where $\eta = \mathrm{col}(x, y, \theta_1, \theta_2)$ is the joint state variable previously defined, the matrix C_η is as defined in (40)-(41), and P_1^B is the boundary projection operator defined in Burns et all.[5] We seek linear combinations of the basis vectors ξ_k, $k = 1, \ldots, 12$, that are in the null-space of the operator $\mathcal{C}$ defined in (51); these then will satisfy the constraints (16)-(17): $\mathcal{C}(\sum_{k=1}^{12} \alpha_k \ \xi_k) = \sum_{k=1}^{12} \alpha_k \ \mathcal{C}(\xi_k) = 0 \in \mathbb{R}^6$. That is, the coefficient vector $\alpha \doteq (\alpha_1, \ldots, \alpha_{12})^T \in \mathbb{R}^{12}$ must lie in the null space of the (6×12) matrix whose columns are $\mathcal{C}(\xi_1)$, $\mathcal{C}(\xi_2)$,...,$\mathcal{C}(\xi_{12})$. It can be shown that the six linear combinations of $\{\xi_k\}_{k=1}^{12}$ that satisfy the constraint (16)-(17) are:

$$(*)\left\{\begin{array}{l} -2\xi_{10}+\xi_{11}-2\xi_{12} \\ -2\xi_7+\xi_8-2\xi_9 \\ \xi_4+\frac{1}{2}[(-\frac{1}{b_2}+\ell_2)\xi_{10}+(\frac{1}{b_2}+\ell_2)\xi_{12}] \\ \xi_3+\frac{1}{2}[(-\frac{1}{b_1}+\ell_1)\xi_7+(\frac{1}{b_1}+\ell_1)\xi_9] \\ \xi_2-\cos\varphi_1\xi_5+\cos\varphi_2\xi_6+\frac{\sin\varphi_1}{2}(\xi_7+\xi_9)+\frac{\sin\varphi_2}{2}(\xi_{10}+\xi_{12}) \\ \xi_1-\sin\varphi_1\xi_5-\sin\varphi_2\xi_6-\frac{\cos\varphi_1}{2}(\xi_7+\xi_9)+\frac{\cos\varphi_2}{2}(\xi_{10}+\xi_{12}) \end{array}\right.$$

where $b_i \doteq \left(b_{N-2}^{(i)}\right)'(L_i)$, $i=1,2$. Now, we choose a basis $\mathcal{S}_c^N=\{\mathbf{b}_1,\ldots,\mathbf{b}_{4N-4}\}$ for our finite-dimensional constrained configuration space $\mathcal{H}_c^N \doteq \text{span}(\mathcal{S}_c^N)\subset\mathcal{H}_u$:

$$\mathbf{b}_i=\begin{bmatrix}0\\0\\l_{i+1}^{(1)}\\0\\\mathbf{0}\end{bmatrix},\quad i=1,\cdots,N-2,\quad \mathbf{b}_{N-2+i}=\begin{bmatrix}b_i^{(1)}\\0\\0\\0\\\mathbf{0}\end{bmatrix},\quad i=1,\cdots,N-3,$$

and the remaining basis elements are chosen so as to satisfy $(*)$.

For the sake of simplicity, in what follows, no internal joint moment effects will be considered, i.e., we assume $b=k=0$ and therefore $M_Q(t)\equiv 0$ (see equation (13)). Using the weak formulations of equations (1)-(3)-(9)-(10)-(11)-(12) with test functions $\mathbf{\Phi}=(\Phi^1,\Phi^2,\Phi^3,\Phi^4,\Phi^J)^T\in\mathcal{H}_c^N\subset\left(L^2(0,L_1)\times L^2(0,L_2)\right)^2\times\mathbb{R}^4$, integrating by parts and using boundary conditions (2) and (4), leads to the weak-form

$$\begin{aligned}\rho_1A_1\left[\langle w_{tt}^1,\Phi^1\rangle+\langle u_{tt}^1,\Phi^3\rangle\right]+\rho_2A_2\left[\langle w_{tt}^2,\Phi^2\rangle+\langle u_{tt}^2,\Phi^4\rangle\right]+\langle M_\eta\ddot{\eta},\Phi^J\rangle_{\mathbb{R}^4}\\+\langle E_1I_1w_{ss}^1+\gamma_1w_{sst}^1,\Phi_{ss}^1\rangle+\langle E_2I_2w_{ss}^2+\gamma_2w_{sst}^2,\Phi_{ss}^2\rangle\\+\langle E_1A_1u_s^1+\mu_1u_{st}^1,\Phi_s^3\rangle+\langle E_2A_2u_s^2+\mu_2u_{st}^2,\Phi_s^4\rangle+\langle\mathcal{C}\mathbf{\Phi},F\rangle_{\mathbb{R}^6}=0\ ,\end{aligned}\quad (52)$$

where $\mathcal{C}$ is the operator defined in (51), F is as given in (40), and M_η is the matrix defined in (38). Here, $\langle\ ,\ \rangle_{\mathbb{R}^6}$ refers to the inner-product in $\mathbb{R}^6$, while $\langle\ ,\ \rangle$ refers to the L_2 inner-product.

Following the usual Galerkin procedure, we use the basis $\{\mathbf{b}_1,\ldots,\mathbf{b}_{4N-4}\}$ both to approximate the solution

$$\begin{bmatrix}w^1(t)\\w^2(t)\\u^1(t)\\u^2(t)\\\eta(t)\end{bmatrix}\approx\sum_{j=1}^{4N-4}z_j(t)\mathbf{b}_j\ ,$$

and also as test functions $\mathbf{\Phi}$. We use the notation $\mathbf{b}_j=\left(\mathbf{b}_j^1,\mathbf{b}_j^2,\mathbf{b}_j^3,\mathbf{b}_j^4,\mathbf{b}_j^J\right)^T$, $j=1,2,\ldots,4N-4$. Note that in this setting the last term in (52) vanishes since by construction the basis vectors satisfy $\mathcal{C}\mathbf{b}_j=0\in\mathbb{R}^6$.

This leads to the finite-dimensional model

$$M^N \ddot{z}^N(t) + D^N \dot{z}^N(t) + K^N z^N(t) = 0 \in \mathbb{R}^{4N-4} \, , \tag{53}$$

where the $(4N-4) \times (4N-4)$ matrices are given by:

$$\begin{aligned} M^N_{i,\,j} &= (\rho_1 A_1) \left[\langle \mathbf{b}^1_j, \mathbf{b}^1_i \rangle + \langle \mathbf{b}^3_j, \mathbf{b}^3_i \rangle \right] \\ &+ (\rho_2 A_2) \left[\langle \mathbf{b}^2_j, \mathbf{b}^2_i \rangle + \langle \mathbf{b}^4_j, \mathbf{b}^4_i \rangle \right] + \langle M_\eta \mathbf{b}^J_j, \mathbf{b}^J_i \rangle_{\mathbb{R}^4} \end{aligned} \tag{54}$$

$$\begin{aligned} K^N_{i,\,j} &= (E_1 I_1) \left[\langle (\mathbf{b}^1_j)'', (\mathbf{b}^1_i)'' \rangle \right] + (E_2 I_2) \left[\langle (\mathbf{b}^2_j)'', (\mathbf{b}^2_i)'' \rangle \right] \\ &+ (E_1 A_1) \left[\langle (\mathbf{b}^3_j)', (\mathbf{b}^3_i)' \rangle \right] + (E_2 A_2) \left[\langle (\mathbf{b}^4_j)', (\mathbf{b}^4_i)' \rangle \right] \end{aligned} \tag{55}$$

$$\begin{aligned} D^N_{i,\,j} &= \gamma_1 \left[\langle (\mathbf{b}^1_j)'', (\mathbf{b}^1_i)'' \rangle \right] + \gamma_2 \left[\langle (\mathbf{b}^2_j)'', (\mathbf{b}^2_i)'' \rangle \right] \\ &+ \mu_1 \left[\langle (\mathbf{b}^3_j)', (\mathbf{b}^3_i)' \rangle \right] + \mu_2 \left[\langle (\mathbf{b}^4_j)', (\mathbf{b}^4_i)' \rangle \right] \; . \end{aligned} \tag{56}$$

4 NUMERICAL RESULTS

We present first some numerical results obtained with the geometric approach described in section 3.2. Initially, we compare our numerical approximation to *exact* results from [6, see pages 431, 432]. For this purpose we specify some geometric and material properties of the beams in Table 1.

Table 1: Beam parameters

Parameter	Value
Length	1.22555 m
Diameter	0.1054 m
Thickness	0.0015 m
Material Density	1149 $\mathrm{kg/m^3}$
Young's Modulus	$0.9\ 10^{11}\ \mathrm{N/m^2}$

Table 2: Low-inertia joint parameters

Parameter	Value
leg mass	0.2797 mg
leg length	1.22555 mm
pin mass	0.1399 mg

With these properties the mass of the beam is 0.6993 kg. For the current comparison we specify joint parameters in Table 2. With these values the joint mass is 10^{-6} that of the beam, with 40 % of the joint mass in each leg, and 20 % in the pin. The length of a joint leg is 0.1 % of the beam's length, and the center of mass of the joint leg is at its mid-point. Thus, the joint-inertia terms are quite small.

We took $N^u_1 = N^u_2 \doteq N^u$ and $N^w_1 = N^w_2 \doteq N^w$. As noted above, the *exact* values in Table 3 are from D. Hartog.[6] Specifically, listed as modes 1 and 3 are first two transverse modes of a *clamped-free* beam; listed modes 2 and 4 are the first two transverse modes of a *clamped-pinned* beam; and, listed mode 5 is the first axial mode of a *clamped-free* beam. In our computed mode-shapes, modes $1-4$ exhibit virtually no axial motion, while mode 5 has no transverse motion. Additionally, modes 1 and 3, show non-zero transverse end-displacement and equal end-slopes, while modes 2 and 4, show zero transverse end-displacement and opposite end-slopes. Lastly, the transverse modal frequencies from[6] are given to only 2 or 3 digits. We conclude that the results from our MATLAB code are reasonable.

Table 3: Comparison with *exact* results

N^u	N^w	ω_1	ω_2	ω_3	ω_4	ω_5
2	8	771.9	3378.5	4838.4	10957.3	11636.9
4	8	771.9	3378.5	4838.4	10957.3	11416.6
8	8	771.9	3378.5	4838.4	10957.3	11361.8
16	8	771.9	3378.5	4838.4	10957.3	11348.1
32	8	771.9	3378.5	4838.4	10957.3	11344.7
32	32	771.9	3378.3	4837.6	10947.8	11344.7
64	64	771.9	3378.5	4838.4	10957.3	11343.9
exact		773	3380	4830	10980	11343.6

4.1 Equilateral configuration

The numerical approximation procedures are now applied to a two-beam system with $\varphi_1 = \varphi_2 = 60^o$ (an equilateral configuration). Beam parameters are as given in Table 1 while nominal joint parameters are given in Table 4. The mass of the joint is 20 % that of the beam, and is distributed as described above. The length of a joint leg is 10 % of the beam's length, and the center of mass of the joint leg is at its mid-point.

Table 4: Nominal joint parameters

Parameter	Value
leg mass	55.94 g
leg length	.122555 m
pin mass	27.97 g

4.2 Undamped Frequencies

As an initial exercise, we study mesh-convergence of modal frequencies for the undamped system. Once again we took $N_1^u = N_2^u \doteq N^u$ and $N_1^w = N_2^w \doteq N^w$. Note that our software implementation requires that $N^w > 6$. From Table 5, we conclude that $N^u = 16, N^w = 16$ provides reasonable accuracy. Modal shapes for the first four frequencies (using $N^u = N^w = 32$) are shown in Figures 3-6. It can be seen that the first mode involves rotation ($\theta_1 = \theta_2 = -1$) and *vertical* translation ($y = -0.0477$) of the joint, but very little x motion. The beams move up and down in concert, when beam-1 is in compression, beam-2 is in tension. The second mode displays small *horizontal* translation. The bending motions are perfectly out-of-phase; both moving outward or both moving inward, while the axial motions are perfectly in-phase. In the third mode the beam motions are similar to the first, but the joint translation (y) is much greater. The fourth mode is similar to the second; bending motions are in-phase, while axial motions

Table 5: Mesh convergence

N^u	N^w	ω_1	ω_2	ω_3	ω_4
2	8	2721	2801	7285	8852
4	8	2721	2801	7273	8838
8	8	2721	2801	7269	8834
16	16	2721	2801	7267	8829
32	32	2721	2801	7267	8829
64	64	2721	2801	7267	8829

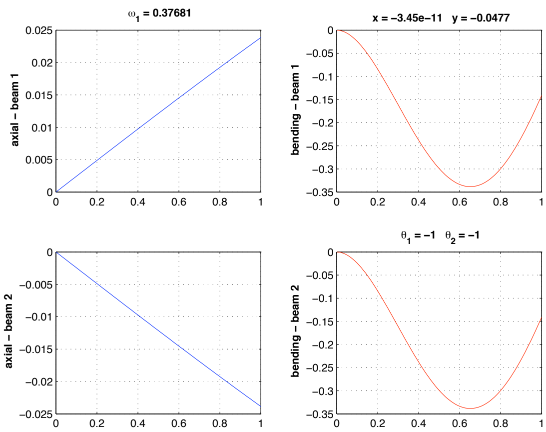

Figure 3: 1^{st} mode

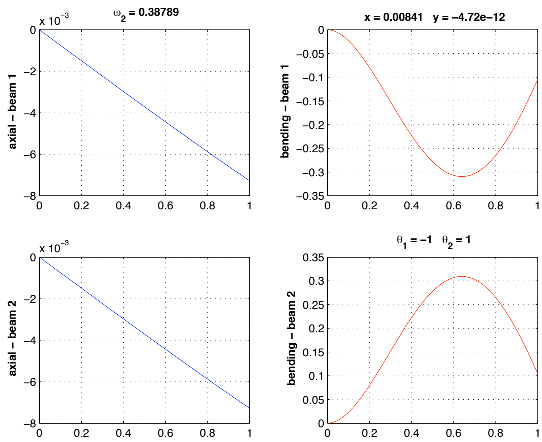

Figure 4: 2^{nd} mode

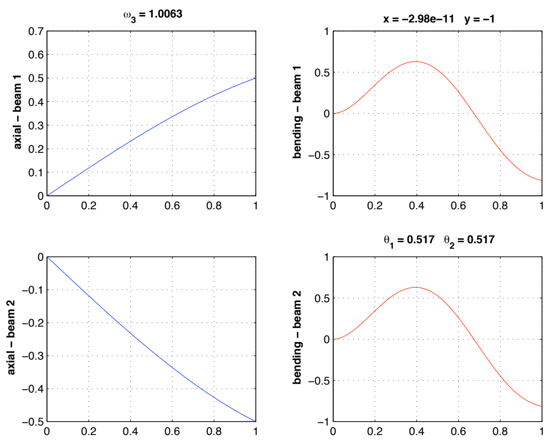

Figure 5: 3^{rd} mode

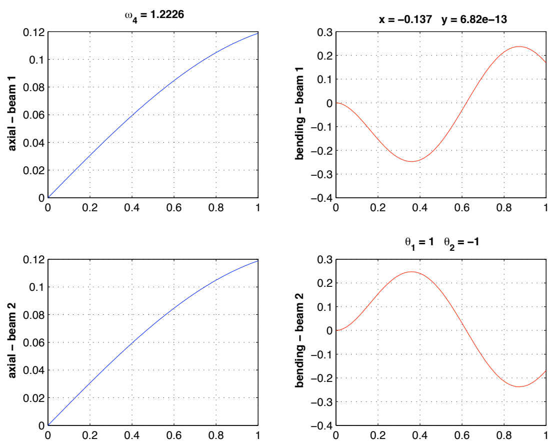

Figure 6: 4^{th} mode

are out-of-phase. Here, again, joint translation (x) is larger than in the second mode. Note that the frequency labels in these figures are based on dimensionless time. The natural time unit, suggested by the axial equation, is given by $tu \doteq L\sqrt{\rho/E}$ and evaluates to .138474496 ms.

Next, we study the effects of the joint-mass parameter on the first few modal frequencies. In each case, each joint-leg is 40 % of the joint-mass, while the pin is 20 %. In these calculations we used $N^u = N^w = 32$. Recall that the latter two modes exhibit more joint translational

Table 6: Joint mass effect

Joint Mass	ω_1	ω_2	ω_3	ω_4
10^{-6}	2739	2809	8116	9065
.001	2739	2809	8113	9064
.010	2738	2809	8077	9056
.050	2735	2807	7913	9017
.100	2730	2805	7699	8963
.200	2721	2801	7267	8829
.500	2692	2789	6169	8208

motion than the first two; thus, it seems reasonable that these modal frequencies depend more strongly on the joint mass.

4.3 Damping Ratio

The damping characteristics, parameterized by the constants μ_1, μ_2, γ_1 and γ_2 in our model, are arguably the most troublesome to estimate. Initially, we take $\mu_1 = \mu_2 \doteq \mu = 10\,\mathrm{kg\ m/s}$, $\gamma_1 = \gamma_2 \doteq \gamma = 0.1\,\mathrm{kg/s}$. We compute eigenvalues of the system (approximated by $N^u = N^w = 32$).

Figure 7 shows the distribution of the eigenvalues. Figures 8 and 9 have been truncated to highlight lower frequencies. Note that most of these eigenvalues are nearly repeated roots. It appears that in one of the modes the bending motions of the beams are identical and nearly in-phase, while the axial motions are identical and nearly 180º out-of-phase. The other mode at nearly the same frequency and damping has identical, nearly in-phase axial motions and identical, nearly 180º out-of-phase bending motions. Table 7 shows the modal damping parameter in the first four modes for several values of the damping parameters μ and γ. It appears that the axial damping parameter (μ) has little effect on the first four modes, while the damping ratios vary approximately linearly with the transverse damping parameter (γ).

4.4 Response to initial data

Our final numerical study is solution of an initial value problem for the two-beam system. For given values of the joint displacements (*i.e.* x, y, θ_1, θ_2) we compute the compatible values of the beam end-conditions (*i.e.* $u^1(L_1)$, $u^2(L_2)$, $w^1(L_1)$, $w^1_s(L_1)$, $w^2(L_2)$, $w^2_s(L_2)$). Assuming a linear distribution of axial beam displacement, and a cubic distribution of bending displacement

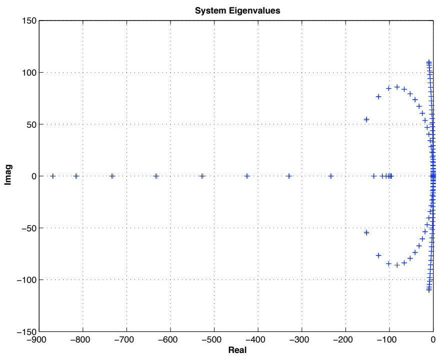

Figure 7: Eigenvalue Distribution

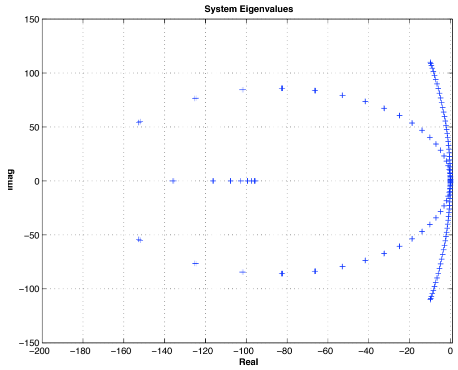

Figure 8: Eigenvalue Distribution (close-up)

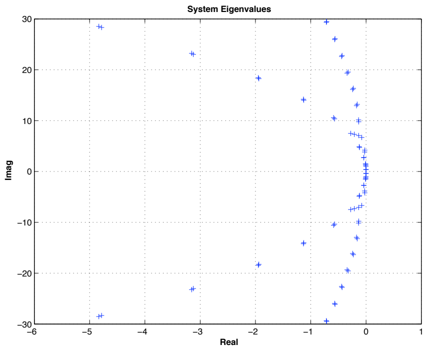

Figure 9: Eigenvalue Distribution (close-up)

Table 7: Damping parameter survey

μ	γ	ζ_1	ζ_2	ζ_3	ζ_4
1	.1	0.0020	0.0022	0.0023	0.0053
10	.1	0.0021	0.0022	0.0028	0.0055
50	.1	0.0021	0.0023	0.0048	0.0065
10	.2	0.0041	0.0045	0.0050	0.0107
10	.5	0.0102	0.0112	0.0117	0.0266
10	1	0.0204	0.0224	0.0228	0.0538

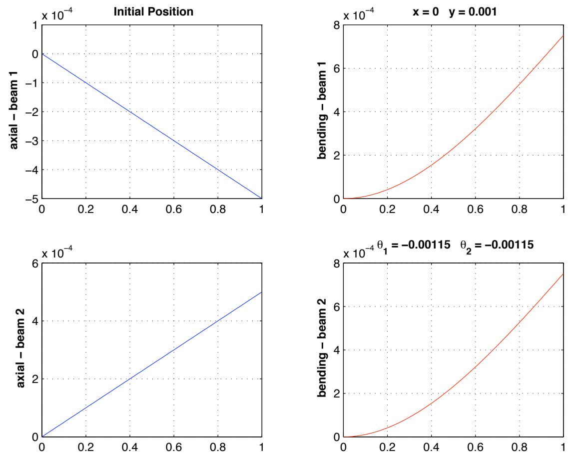

Figure 10: Initial displacement

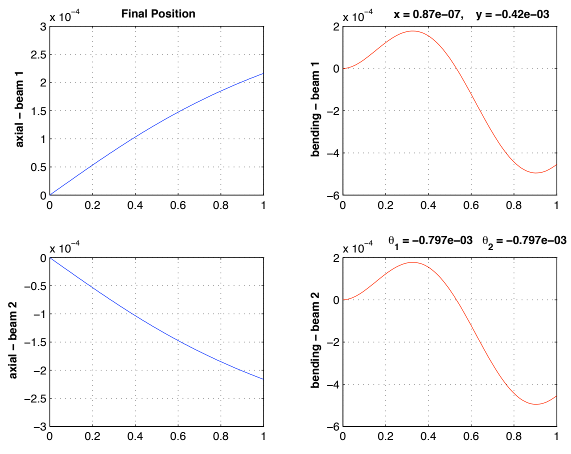

Figure 11: Final displacement

(along with the boundary conditions $u^1(0) = w^1(0) = w^1_s(0) = u^2(0) = w^2(0) = w^2_s(0) = 0$) we can solve uniquely for the axial and bending distributions. With these in hand, the strain energy can be evaluated.

For the initial displacement of the two-beam system, we specify $x = 0$, $y = 1\ mm$ and compute values θ_1 and θ_2 so as to minimize the initial strain energy, using the linear/cubic beam shapes as noted above. Figure 10 displays the initial deflections of the beams. Note that with y positive the upper beam is in compression, while the lower beam is in tension. Both beams exhibit positive bending displacements. Figure 12 displays the time history of the joint translation; the simulation maintains $x = 0$, as expected. Figure 11 displays the final deflections of the beams (at $t = 0.01\ s$). The anti-symmetry of the axial displacements has been preserved, while the bending displacements remain in-phase. Note that the axial displacement indicates non-uniform strain (*i.e.* u_ξ is not constant). Figure 13 shows the time history of the total mechanical energy. Approximately one-half of the energy is dissipated in the first 0.01 sec. Figure 14 shows the energy partition among axial (beam 1-kinetic plus potential), bending (beam 1-kinetic plus potential) and joint motions. The energy values are normalized by the total instantaneous energy, so the total should be unity. Perhaps the most surprising feature is that, at times, the joint carries up to 40% of the total energy.

Finally we present some numerical results obtained with the projection method described in Section 3.1.1. Figures 15, 16, 17 show the distribution of the eigenvalues obtained with this method. We observed that they are almost identical to those obtained with the previous method. Similarly, Figure 18 shows the time evolution of the joint's tip obtained with this method for the same initial conditions described in Section 4.4.

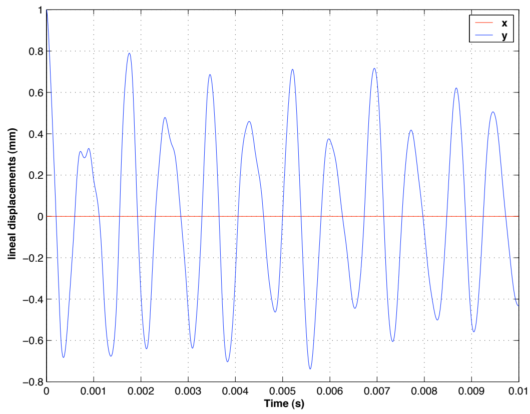

Figure 12: Joint displacement history

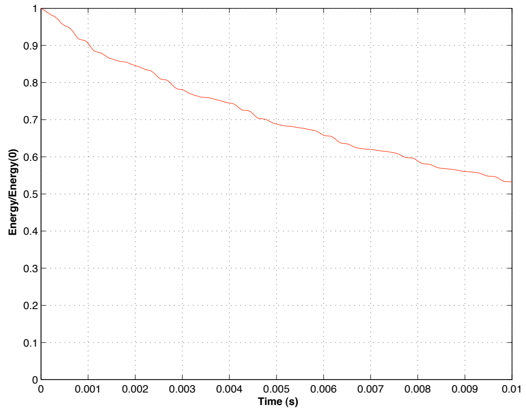

Figure 13: Energy history

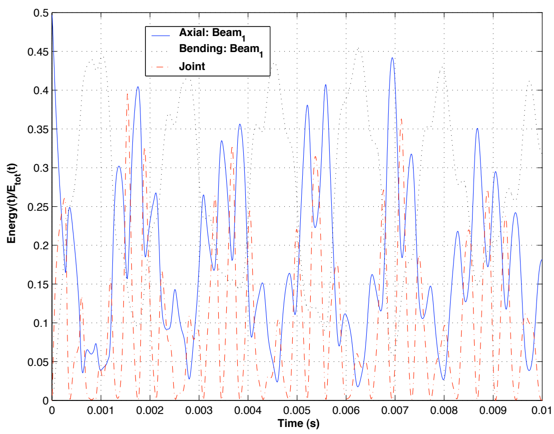

Figure 14: Energy partition

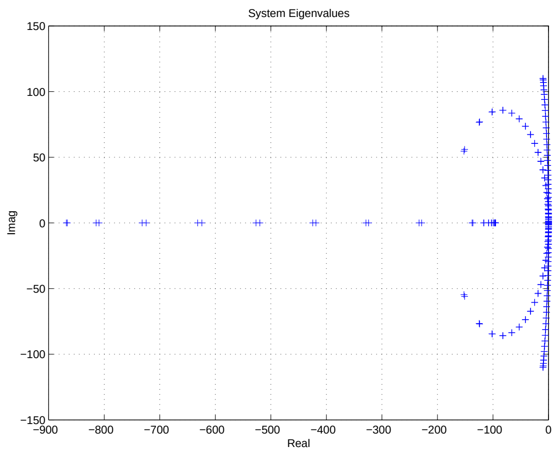

Figure 15: Eigenvalue distribution, projection method

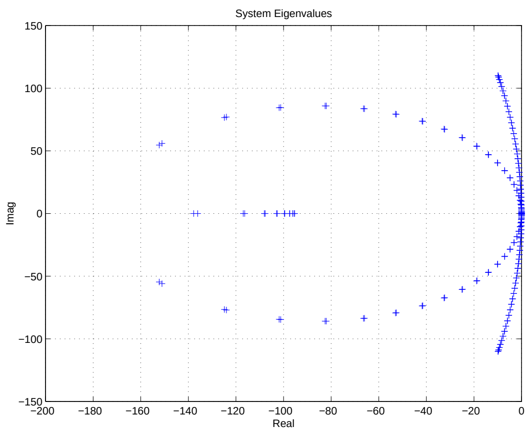

Figure 16: Eigenvalue distribution, projection method (close up)

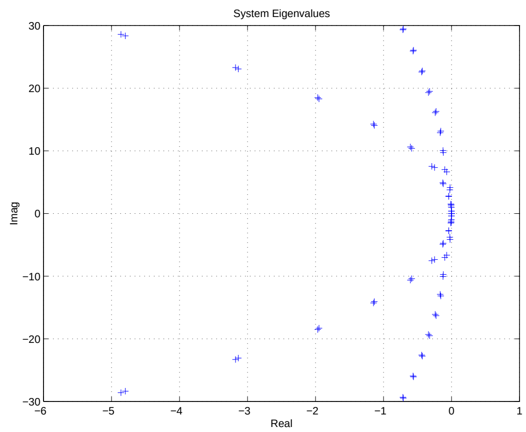

Figure 17: Eigenvalue distribution, projection method (close up)

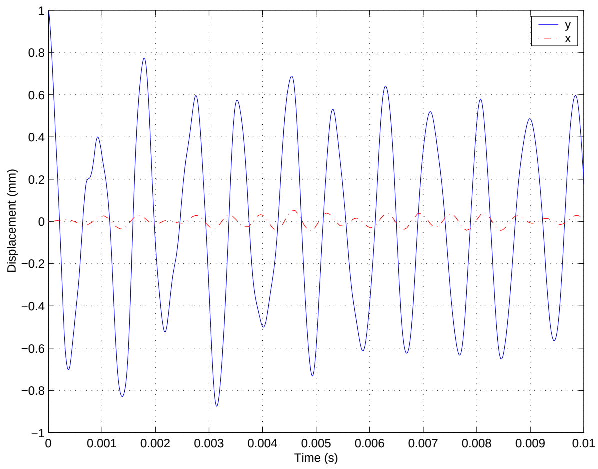

Figure 18: Evolution of the joint, projection method

5 CONCLUSIONS

In this article, a model for the dynamics of tow beams with Kelvin-Voigt damping, coupled to a joint through two legs was presented. The total energy of the system was computed and its dissipativeness was shown. Two different approaches were followed to develop finite dimensional approximations for the solutions of the system. One approach used a projection method to enforce the dynamic boundary conditions while the other consisted of enforcing these boundary conditions into the basis functions. Numerical results were presented for both methods. Frequency and damping characteristics were analyzed and the response of the system to initial data was studied.

REFERENCES

[1] C. H. M. Jenkins (ed.), *Gossamer Spacecraft: Membrane and Inflatable Structures Technology for Space Applications*, Progress in Aeronautics and Astronautics Series, 191, AIAA Publications, 2001.

[2] J. E. Lagnese, G. Laugering and E. J. P. G. Schmidt, *Modeling, Analysis and Control of Dynamic Elastic Multi-Link Structures*, Birkhäuser, 1994.

[3] J. A. Burns and B. B. King, *A Note on the Mathematical Modelling of Damped Second Order Systems*, Journal of Math. Systems, Estimation and Control, Vol. 8, No.2, 1998, pp 189-192.

[4] K. Liu and Z. Liu, *Analyticity and Differentiability of Semigroups Associated with Elastic Systems with Damping and Gyroscopic Forces*, J. Differential Equations, Vol. 141, 1997, No. 2, pp 340-355.

[5] J.A. Burns, E.M. Cliff, Z. Liu and R. D. Spies, *On Coupled Transversal and Axial Motions of Two Beams with a Joint*, submitted.

[6] J.P. Den Hartog, Mechanical Vibrations, *Fourth Ed.*, McGraw-Hill, 1956.